A high linear silicon Mach-Zehnder modulator by the dual-series architecture

Qiang Zhang, Hui Yu, Zhilei Fu, Penghui Xia, Xiaofei Wang
Institute of Integrated Microeletronic Systems, College of Information Science and Electronic Engineering, Zhejiang University, Hangzhou 310027, China, zhangqiang863@zju.edu.cn

Abstract: We experimentally demonstrate a highly linear dual-series silicon modulator by tuning properly the power splitting ratio of the driving RF signal on the its two sub-MZMs, with SFDR of 109.5/100.5 dB·Hz$^{2/3}$ at 1/10 GHz. © 2020 The Author(s)
OCIS codes:(130.0130) Integrated optics; (060.5625) Radio frequency photonics

1. Introduction

A mainly important performance metric on a microwave photonics (MWP) link is linearity which is characterized by the spurious-free dynamic range (SFDR). It is known that the dominating nonlinear distortion of the MPL is mainly induced by the electro-optical (EO) modulator. Thanks to the rapid progress of silicon photonics made in last decades, therefore, highly linear silicon modulators, especially based on Mach-Zehnder architecture with the advantages of larger optical bandwidth and insensitivity to temperature fluctuation, are strongly desired by integrated silicon MWP systems. Due to the lack linear EO effect on silicon, most silicon MZMs employ the plasma dispersion effect and the carrier-depletion mechanism to change refractive indexes to final optical intensity modulations. A lot of efforts have been made to linearize the silicon MZMs [1-3]. All the mentioned methods to improve the linearity of silicon MZMs rely on the processing flows and materials that are not CMOS compatible. On the other hand, the linearity of MZM can also be improved by cascading two sub-MZMs in parallel or series, which have been proved to be effective in $LiNbO_3$ platform [4,5]. It is also applicable to silicon MZMs in principle. The dual-parallel high linear silicon MZMs has been reported in [6]. Here, we demonstrate a highly linear all-silicon MZM based on dual-series configuration. Compared with the dual-parallel silicon MZM in [6], our device only requires less control variables and presents a higher linearity. The measured SFDR for the third inter-modulation distortion (IMD3) are as high as 109.5/100.5 dB·Hz$^{2/3}$ at 1/10 GHz. Finally, we design and simulate a novel dual-series architecture to further decrease the complexity of the operation.

2. Device Architecture & Linearization Principle

A schematic diagram and a microscope image of our device are shown in Figs. 1(a) and 1(b), respectively. It composed of two identical silicon carrier-depletion-based MZ modulators which are connected in series. Phase shifters of the two MZMs are 500-μm-long rib waveguides with embedded PN junctions. Dimension and etching depth of rib waveguides are 450 nm × 220 nm and 150 nm, respectively. The nominal doping concentration of the PN junction is 1×10^{18} / cm^3. The ohmic contact regions are heavily doped to 10^{20} / cm^3 to reduce the contact resistance. Doped silicon strips at both sides of the waveguide act as heaters to set bias points of the two MZMs. Cross-sections of the phase shifter and the heater are shown in Fig. 1(c) and 1(d), respectively. Devices are fabricated by joining the silicon photonics MPW service of IMEC (ISIPP50G) [7].

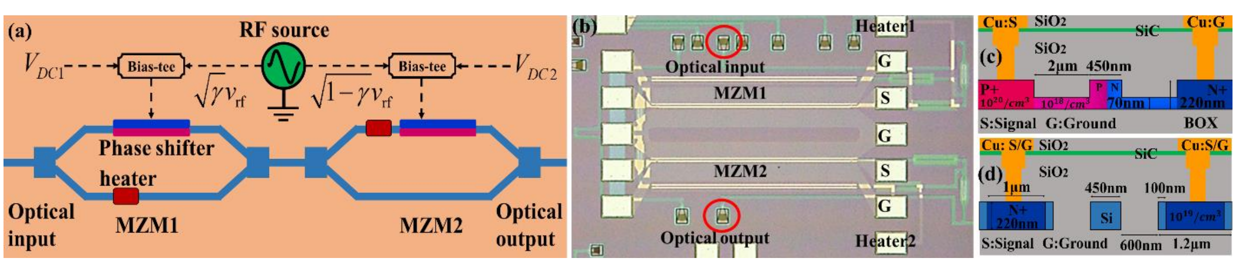

Fig. 1(a) Schematic diagram of the silicon dual-series MZM. (b) Microscope image of the silicon dual-series MZM. Cross-sectional views (c) the PN junction and (d) the heater of the silicon MZMs.

The modulation transfer function of dual-series MZM in Fig. 1 is the product of the individual transfer functions of the two sub-MZMs, which can be written as [8]

$$I_{\text{dual-series}} = \frac{\left|E_{\text{in}}\right|^2}{16}\begin{bmatrix} e^{-2\alpha(0)L} + e^{-2\alpha(\sqrt{\gamma}v_{\text{rf}}+V_{\text{DC1}})L} \\ +2e^{-(\alpha(0)+\alpha(\sqrt{\gamma}v_{\text{rf}}+V_{\text{DC1}}))L}\cos\left(\Phi_1\right) \end{bmatrix} \cdot \begin{bmatrix} e^{-2\alpha(0)L} + e^{-2\alpha(\sqrt{1-\gamma}v_{\text{rf}}+V_{\text{DC2}})L} \\ +2e^{-(\alpha(0)+\alpha(\sqrt{1-\gamma}v_{\text{rf}}+V_{\text{DC2}}))L}\cos\left(\Phi_2\right) \end{bmatrix} \quad (1)$$

In Eq. (1), $|E_{\text{in}}|^2$ represents the power of input optical field, $\alpha(v)$ is the attenuation coefficient of the phase shifter which depends on the driving voltage v on the PN junction. $\Phi_{1/2}$ denote optical path differences between two arms of the two sub-MZMs, which can be calculated as $\Phi=\Phi_{\text{bias}}+2\pi L\Delta n_{\text{eff}}(v)/\lambda$. Here Φ_{bias} represents the static bias phase produced by the heater, $\Delta n_{\text{eff}}(v)$ represents the effective index change induced by the driving voltage v. Considering the splitting ratio of the RF power on the two sub-MZ is γ: $(1-\gamma)$, driving voltages on the two sub-MZMs are $V_{\text{DC1}} + \sqrt{\gamma}v_{\text{rf}}$ and $V_{\text{DC2}} + \sqrt{1-\gamma}v_{\text{rf}}$. Here, V_{DC} and v_{rf} denote the static reverse bias voltage applied on the PN junction and the output of the RF signal source. In our scheme, both sub-MZMs operate at their quadrature points, but with opposite polarities, i.e., $\Phi_{\text{bias1}}+2\pi L\Delta n_{\text{eff}}(V_{\text{DC1}})/\lambda=\pi/2$, $\Phi_{\text{bias2}}+2\pi L\Delta n_{\text{eff}}(V_{\text{DC2}})/\lambda=-\pi/2$. According to the nonlinear modulation theory [8], amplitudes of the first harmonic (FH) and the IMD3 components in the modulated optical field can be obtained by calculating derivatives of $I_{\text{dual-series}}$ with respect to v_{rf}. With a proper value of the splitting ratio γ, the IMD3 component can be suppressed.

3. Experiments and Results

The two-tone test is implemented to characterize linearities of the two devices with the measurement setup shown in Fig. 2. TE polarized light at a wavelength of 1550 nm from a continuous wave (CW) tunable laser (Santec TSL-710) is coupled into and out of the chip by two fiber grating couplers. The driving two-tone signal is generated by a RF source (Keysight E8267D), and then is equally distributed to two paths by a 50/50 RF power splitter. One path is connected to an electrical attenuator (EA) to control the power ratio of the RF driving singles on the two sub-MZMs, while the other path goes through an electrical phase shifter (EPS) to make sure time delays of the two paths are equal. A two-channel voltage source provides reverse bias voltages for PN junctions. The DC bias voltages are combined with the RF driving signals by two bias-tees, and then are fed to the two sub-MZMs by a 50 GHz GSGSG probe. Another two-channel voltage source provides driving currents for heaters. The output of the modulator is amplified by an erbium doped fiber amplifier (Amonics AEDFA-PA-35-B-FA) so as to compensate the coupling loss of the two fiber grating couplers (8 dB in total) and the insertion loss of the device. An optical bandpass filter (OBPF WaveShaper 2000A) is used to suppress the amplified spontaneous emission noise (ASE).

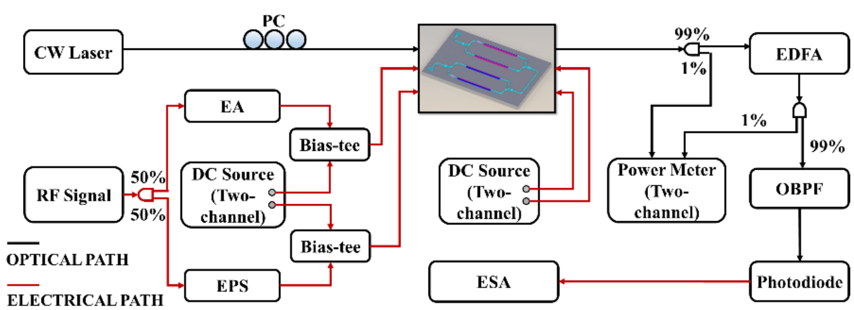

Fig. 2. Setup for the SFDR measurement. CW Laser: continuous wave tunable laser; EDFA: erbium doped fiber amplifier; OPBF: optical bandpass filter; ESA: electrical spectrum analyzer; PC: polarization controller; EA: electrical attenuator; EPS: electrical phase shifter; DUT: device under test.

In order to compare linearities of the single and the dual-series MZMs fairly, their outputs are amplified to 10 dBm. Two 1/99 optical power splitters and a two-channel optical power meter are used to monitor the optical power at the points before and after the EDFA. The first monitoring point enables us to set bias points of MZMs, while the second monitoring point is used to control the output level of the EDFA at 10 dBm during the SFDR measurement. The two tones with a spacing of 10 kHz are centered at 1 GHz or 10 GHz. The noise floors measured by the spectrum analyzer are 156 dBm/Hz and 152 dBm/Hz when the frequency center of the two tones locates at 1 GHz and 10 GHz, respectively. The optical-to-electrical conversion is performed by a 30 GHz photodiode with a responsivity of 0.75 A/W. The output RF signal of the PD is analyzed by a 67 GHz electrical spectrum analyzer (ROHDE&SCHWARZ FSWP).

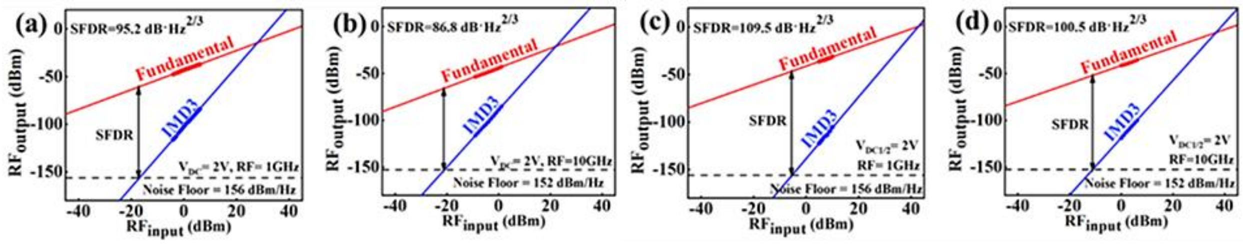

Fig. 3. Measured SFDRs of the dual-series MZM at different driving conditions and frequencies. (a) single drive at 1 GHz. (b) single drive at 10 GHz. (c) dual drive at 1GHz and (d) dual drive at 10 GHz.

The dual-series MZM is characterized at first by biasing the first and the second sub-MZMs at the quadrature and the maximum transmission points, respectively. The RF driving signal is delivered only to the first sub-MZM. The reverse bias voltage on its PN junction is V_{DC}=2 V. The device hence operates as a single-MZM which is subjected to ~1.5 dB additional loss induced by the second sub-MZM. As shown in Figs. 3(a) and 3(b), SFDRs of the device under this driving condition are 95.2/86.8 dB·Hz$^{2/3}$ at 1/10 GHz. After that, the dual-series MZM is characterized by biasing both sub-MZMs at quadrature points and driving them with different RF powers. Reverse bias voltages on both sub-MZMs are set to be V_{DC1}=V_{DC2}=2 V. The splitting ratio γ of the RF power is controlled with the aid of the EA. When the value of γ is tuned to be ~0.8, SFDRs are improved substantially to 109.5 dB·Hz$^{2/3}$ and 100.5 dB·Hz$^{2/3}$ at frequencies of 1 GHz and 10 GHz, respectively.

4. Conclusion

We improve the linearity of silicon carrier-depletion-based modulator by cascading two MZMs in series. A highly linear silicon dual-series MZM is demonstrated with SFDRs of 109.5/100.5 dB·Hz$^{2/3}$ at 1/10 GHz, which is among the highest linearities ever achieved with all-silicon MZMs. Here we want to stress that SFDR is a link metric. It depends not only on the modulation linearity, but also on gain and noise figure of the EDFA, relative intensity noise (RIN) of the laser, and other link parameters. For example, if a low RIN laser is used to suppress the noise floor the link, the measured SFDR would be even higher.

Acknowledgement

The authors would like to thank Dr. Bing Wei, Training Platform of Information and Microelectronic Engineering in Polytechnic Institute of Zhejiang University.

References

[1]. Jianfeng Ding, *et al*. "Method to improve the linearity of the silicon Mach-Zehnder optical modulator by doping control", Opt. Express **24** (21), 24641-24648 (2016).
[2]. C. G. Bottenfield, *et al*. "Silicon Photonic Modulator Linearity and Optimization for Microwave Photonic Links", IEEE J. Sel. Top. Quantum Electron. **25** (5), 1-10 (2019).
[3]. A. Rao, *et al*. "High-performance and linear thin-film lithium niobate Mach–Zehnder modulators on silicon up to 50 GHz", Opt. Letters **41** (24), 5700-5703 (2016).
[4]. S. K. Korotky, *et al*. "Dual parallel modulation schemes for low-distortion analog optical transmission", IEEE J. Sel. Areas in Commu. **8** (7), 1377-1381 (1990).
[5]. G. E. Betts, "Linearized modulator for suboctave-bandpass optical analog links", IEEE Trans. Microwave Theory and Tech., **42** (12), 2642-2649 (1994).
[6]. Y. Zhou, *et al.* "Linearity Characterization of a Dual–Parallel Silicon Mach–Zehnder Modulator", IEEE Photo. Jour. **8** (6), 1-8 (2016).
[7]. M. Rakowski, "Silicon photonics platform for 50G optical interconnects", presented at Proc. Cadence Photon. Summit Workshop 2017, San Jose, USA, 3-4 Sept. 2017.
[8] Q. Zhang, *et al.* "Linearity Comparison of Silicon Carrier-Depletion-Based Single, Dual-Parallel, and Dual-Series Mach–Zehnder Modulators", J. Lightwave Technol. **36** (16), 3318-3331 (2018).